Geotechnical and Geophysical Site Characterisation 5 – Lehane, Acosta-Martínez & Kelly (Eds)

Stochastic Waveform Inversion for Probabilistic Geotechnical Site Characterization

S.S. Parida & K. Sett
Department of Civil Structural and Environmental Engineering, University at Buffalo, New York, United States of America

P. Singla
Department of Mechanical and Aerospace Engineering, University at Buffalo, New York, United States of America

ABSTRACT: This study develops a stochastic inverse analysis methodology to probabilistically estimate site-specific soil modulus from geophysical test measurements by accounting for the uncertain spatial variability of the soil deposit, any measurement uncertainty and uncertainty due to limited data. Hypothesizing the soil modulus to be a three-dimensional, heterogeneous, anisotropic random field, the methodology first formulates and solves a forward model that mimic a geophysical experiment using a stochastic collocation approach to characterize the effect of spatially variable, uncertain soil modulus on the model response variables, for example, accelerations at the sensor locations. The stochastic collocation approach utilizes recently developed non-product quadrature method, conjugate unscented transformation, to accurately estimate statistical moments corresponding to the model response variables in a computationally efficient manner. The methodology then employs a minimum variance framework to merge the information obtained from the model prediction and the sparse geophysical test measurements to update the statistical information pertaining to the soil modulus. The methodology is illustrated using synthetic data from a fictitious geophysical experiment.

1 INTRODUCTION

Quantification of site-specific uncertainties in soil properties through standard geotechnical site characterization approach of drilling and measuring soil properties at a few locations in a soil deposit poses a challenge due to the very limited amount of (borehole) measurements typically available at any geotechnical site. This leads to data uncertainty in the estimation process and it gets carried over unaccounted for in subsequent probabilistic design/simulation of the behavior of geostructures.

Geophysical tests, which are increasingly being used in characterizing geotechnical sites, offer an advantage that they typically yield larger volume of data for more accurate statistical analysis. Traditionally, geophysical test measurements are analyzed deterministically with simplifying assumptions so that the inversion process remains tractable. Spectral analysis of surface waves (SASW) is one such widely used approach that assumes ground waves to consist only of Rayleigh waves and neglects the effects of P- and S-waves (Nazarian 1984). Moreover, it relies on one-dimensional conjecture and hence only produces horizontally layered soil profile (Fathi 2015). In recent years, with advancement of mathematical machineries and availability of faster computers, partial differential equation (PDE) constrained full waveform inversions, which inherently account for all types of waves in a solid medium, have also been successfully attempted to image heterogeneous soil deposits (see, for example, Kallivokas *et al*. 2013). However, such inversion processes, due to their deterministic nature, fail to account for uncertain spatial variability of soil parameters and any measurement uncertainty associated with the geophysical experiments

This paper develops a methodology for PDE-constrained stochastic waveform inversion to not only estimate constitutive parameters of any soil deposit but also to quantify uncertainties associated with them by accounting for uncertain spatial variability and measurement uncertainty as well as uncertainty due to limited data The authors anticipate that such a tool, when properly verified and validated, will tremendously benefit geotechnical engineers in accurately visualizing (in terms of confidence intervals) the heterogeneity of subsurface at any site. This will not only result in more accurate simulation of the behavior of any civil infrastructure objects but also allow for estimation of site-specific resistance factors for the load and resistance factor design (LRFD) of geotechnical components of any civil infrastructure objects. Note that due to very limited amount of soil data typically available at any geotechnical site for a meaningful statistical analysis, the current American Association of State Highway and Transportation Officials (AASHTO) recommended LRFD resistance factors for substructures were derived by just calibrating the LRFD equation

to the factors of safety used in the past with the working stress design (WSD) approach. The factors are indifferent to any site-specific information e.g., variability of soil properties at a particular site, the extent of soil exploration (little versus extensive), etc. The anticipated ability to compute fully site-specific resistance factors will lead to safer and more economical designs of civil infrastructure objects.

2 PROBLEM STATEMENT

We will analyze synthetic data from a fictitious geophysical experiment shown schematically in Figure 1. Assuming a three-dimensional, heterogeneous profile of soil modulus, we will numerically simulate a geophysical experiment to obtain sensor measurements (acceleration/velocity/displacement time histories) due to a known excitation at the source location. We will assume them to represent actual sensor measurements after polluting them a bit by adding Gaussian white noise to mimic real measurements. Finally, using these few measurements and hypothesizing the soil modulus to be a three-dimensional random field, we will inversely estimate its parameters.

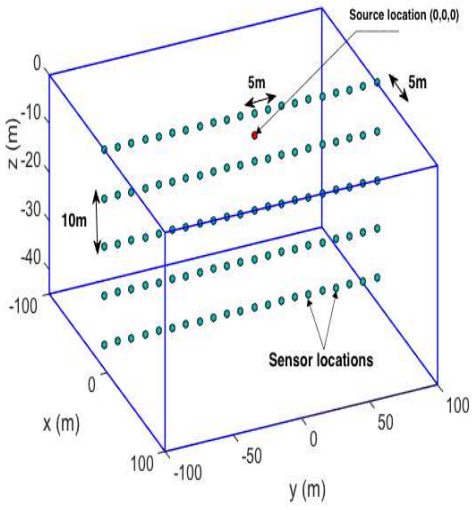

Figure 1. Schematic of the fictitious site to be probed showing sensor and source locations.

3 THE FORWARD PROBLEM

Solution of any PDE-constrained probabilistic inverse problem is, in essence, an iterative process. Each iteration starts with the propagation of the target parameter, with some prior belief about its uncertainties, through the governing PDE ("the model") and then updating the target parameter with the help of a suitable estimator that aims to maximize the likelihood of the observed response by minimizing the error between "the model" predictions and true responses. Thus setting up "the model", propagating prior uncertainties through it and obtaining "the model" response are tantamount to any other stage of the inversion process and constitute the forward problem. In a deterministic setting, forward problems that
are governed by PDEs are typically solved numerically, for example, using the finite element method

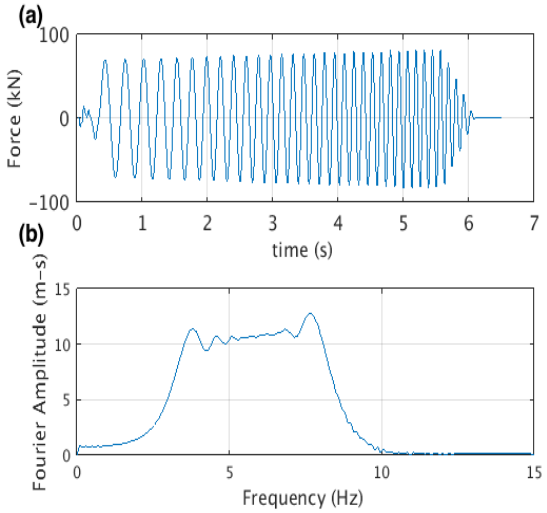

Figure 2. (a) Forcing function at (0,0,0) and (b) its Fourier spectrum

or the finite difference method. In a probabilistic setting where the model parameters are uncertain, the governing PDE becomes a stochastic PDE. Monte Carlo (MC) approach (Doucet *et al* 2001) is the most widely used approach for solving stochastic PDEs. MC approach, in general, is very straightforward and can be used to probabilistically simulate any problem whose deterministic solution – either analytical or numerical – is known. However, its accuracy depends upon the number of realizations (N) used in the simulation process; the MC estimates approach their true values as the number of deterministic runs, N, approaches infinity. Because of the above, accurate probabilistic simulation using MC approach becomes extremely computational intensive, especially for problems which do not have analytical solutions; for large scale problems, like nonlinear dynamic problems in a finite element setting, it will probably be intractable. Among the alternate approaches, the stochastic Galerkin and the stochastic collocation approaches are more common. Stochastic Galerkin approaches (see, for example, Ghanem & Spanos 1991) usually represent all the uncertain parameters of a model using some type of finite series expansions and then employ a Galerkin technique to minimize the errors of finite representation which result in a system of coupled (deterministic) equations. Stochastic collocation approaches (see, for example, Babuska et al. 2007), on the other hand, can be viewed as a Monte Carlo type sampling technique, with the exception that, instead of at random, the sampling points are selected following some kind of numerical quadrature schemes that are

used to estimate the statistical moments of the response variable. Stochastic collocation approaches are, in general, non-intrusive approaches in the sense they do not require modifications of underlying deterministic (finite element or finite difference) code.

This study employs the finite element method in conjunction with the stochastic collocation approach to probabilistically solve the forward problem corresponding to the geophysical experiment shown schematically in Figure 1. The soil deposit is modelled using 8-noded standard brick elements of dimension 5m × 5m × 5m. The horizontal and vertical extents of the soil domain – that theoretically extend to infinity – are restricted by using artificial absorbing boundaries. Widely used Lysmer-Kuhlemeyer (Lysmer and Kuhlemeyer 1969) local boundaries are used for this purpose. A chirp signal (Figure 2) with dominant frequencies between 3Hz and 10Hz was used to excite the ground at the source location for a duration of 6 sec. The soil material is assumed to be linear elastic as the chirp signal is not expected to plastify the soil. While the Poisson's ratio of soil is assumed to be deterministic with a constant value of 0.3 throughout the domain, the Young's modulus of soil is assumed to be a three-dimensional heterogeneous, cross-anisotropic random field.

The random field parameters up to the second order marginal mean values, marginal coefficients of variation (COVs), and vertical and horizontal correlation structures that are the unknowns for the inverse problem – will initially be guessed for the forward simulation. In concurrence with the general soil behavior, marginal mean and COV are assumed to increase with depth. In the horizontal directions, however, they are assumed to be constant. Typically, due to the nature of soil formation process, soil parameters are less correlated in vertical direction than in the horizontal directions (Lacasse & Nadim 1996). Accordingly, the correlation length of Young's modulusin the vertical direction is assumed to be smaller than that in the horizontal directions. It is assumed that there is no correlation between the moduli in x-y plane and vertical direction. Mathematically, we capture the above-assumed spatial variation of uncertain Young's modulus in terms of Gaussian shape functions and weights as:

$$Y(x,y,z) = w_0 + w_1 z + \sum_1^n W_i N_i(\mu_{c_i}, P) \quad (1)$$

$$P = \begin{bmatrix} \sigma & \sigma_{xy} & 0 \\ \sigma_{xy} & \sigma & 0 \\ 0 & 0 & \sigma \end{bmatrix} \quad (2)$$

$$W_i = w_2 r + w_3 \theta \quad (3)$$

where Y is the Young's modulus, μ_{c_i} is the center of each Gaussian shape function and n is the number of Gaussian shape functions. The parameters w_1, w_2, w_3, σ and σ_{xy} are assumed to be random variables that give rise to the uncertainty in Y. z, r and θ are polar coordinates of a spatial point with origin at (0,0,0). The correlation in Y is indirectly captured here by the summation in Equation (1) since we hypothesize that the magnitude of Y at a point in space is a result of all the Gaussians shape functions. With this we can write $\Theta = [w_1, w_2, w_3, \sigma, \sigma_{xy}]$ to be the uncertain parameter vector of the system. Notice that the assumed structure of Eq. (1) on the Young's modulus field allows us to represent a random field with the help of only 6 parameters Assuming uniform distribution for the random vector Θ, we can write it as:

$$\theta_i(\xi) \cong \theta_{i_0} + \theta_{i_1}\xi_i \qquad \forall\ \theta_i \in \Theta \quad (4)$$

where $\boldsymbol{\xi} = [\xi_1, \xi_2, \dots]^T$ is a known vector of uniform random variables. Further, since the acceleration at a spatial location is a function of Y, and given that Y itself is a function of Θ, acceleration at any geospatial location in the domain becomes a function of the random parameter vector Θ. Therefore, the expected value of any scalar function of acceleration, a, can be computed as:

$$\mathcal{E}\left[f\left(a(\Theta)\right)\right] = \int_\Theta f(a(\Theta))p(\Theta)d\Theta \cong \sum_q w_q f\left(a\left(\Theta(\xi_q)\right)\right) \quad (5)$$

where $\Theta(\xi_q)$ is evaluated at quadrature points ξ_q and and w_q are the respective weights. Only values of the response variable corresponding to these quadrature points are necessary to calculate the expectation and hence the model is simulated for values of Y corresponding to those $\Theta(\xi_q)$s. Many quadrature rules ex-ist in the literature of stochastic collocation for choosing the sample points like Gaussian closure (Iyengar & Dash 1978), unscented transform and Smyolak sparse grid quadrature (Nagavenkat 2012). The major problem with these quadrature rules is that they get computationally very expensive as the dimensionality
of the problem increases. Recently, a non-product quadrature rule known as the conjugate unscented transformation (CUT) has been developed (Nagavenkat 2012, Nagavenkat et al 2013, Mandankan 2014, Mandankan et al 2014). The CUT approach can be considered as an extension of the conventional unscented transform method that satisfies additional higher order moment constraints. It uses just a small number of points, relative to the Gauss quadrature scheme, to compute an integral with the same accuracy. Thus, we start by generating 5-dimensional CUT points (and respective weights) corresponding to the 5 random variables w_1, w_2, w_3, σ and σ_{xy} and evaluate their values at these quadrature according to Equation (4). For example, the random variable w_1 can be evaluated as:

$$w_1(\xi_{1q}) = a_0 + a_1\xi_{1q} \quad (6)$$

where ξ_{1q} corresponds to the q[th] quadrature point.

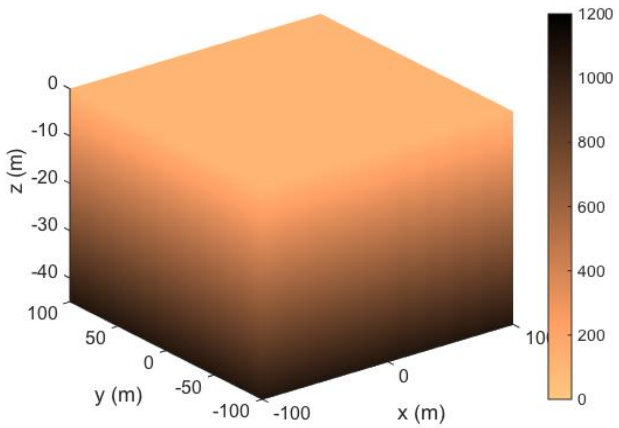

Figure 3. Distribution of true value of Young's modulus (MPa).

Table 1. Coefficients of random variables.

Random Variable	1st coefficient MPa	2nd coefficient MPa
$\boldsymbol{w_1}$	22.4	2
$\boldsymbol{w_2}$	0.035	0.0071
$\boldsymbol{w_3}$	0.79	0.15
$\boldsymbol{\sigma}$	3.70	0.74
$\boldsymbol{\sigma_{xy}}$	3.70	0.74

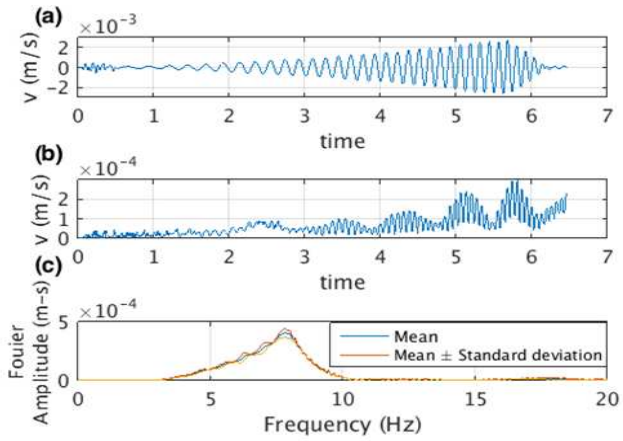

Figure 4. (a) Mean, (b) standard deviation of the simulated velocity time history at (-5,0,0) and (c) corresponding Fourier spectra.

Note that $\boldsymbol{\xi}$ are uniform random variables with zero mean and unit variance. Prior values of coefficients a_0 and a_1 are assumed to be 22.4 MPa and 2 MPa respectively. Similar prior assumptions of other random variables lead to the coefficient values listed in Table 1. We state that the CUT approach needs just 425 quadrature points for our 5-D problem to accurately compute the expectations and hence our model requires as many forward runs, each run corresponding to a realization of Y. For shape functions, we assumed 10 Gaussian functions in each direction initially. Due to much smaller extent of the target domain in the vertical direction this assumption ensures smaller correlation length along it than in horizontal directions. The 3D soil domain corresponding to the true value of Young's modulus is shown in Figure 3. Once the computational model is set up it is run for all the quadrature realizations of Y. Mean and standard deviation of the simulated velocity time history and corresponding Fourier spectra at a node located at (-5,0,0) are shown in Figure 4.

4 THE INVERSION PROCESS

For the inversion process the acceleration time histories recorded at sensor locations are used to compute our posterior moments. To this end, we employ the minimum variance framework (Madankan 2014).

4.1 *Minimum Variance*

Consider a sensor model given by Equation (6), where $h(\Theta)$ corresponds to the true value of the response of the corresponding dynamic system, ν represents the sensor noise with a zero mean and covariance matrix R, and y is the measured response. For such a system, according to the minimum variance framework, the first two posterior moments of the parameter vector Θ, are given by Equations (7) and (8), respectively.

$$y = h(\Theta) + \nu \tag{7}$$

$$\mu_{\Theta}^{+} = \mu_{\Theta}^{-} + K[y - \mathcal{E}^{-}[h(\Theta)]] \tag{8}$$

$$\Sigma_{\Theta}^{+} = \Sigma_{\Theta}^{-} - K\Sigma_{\theta y}^{T} \tag{9}$$

where superscripts – and + denote prior and posterior value of the corresponding random variable. The matrix K is called the Kalman gain matrix and is a measure of the information gained due to the observation y. It is given by:

$$K = \Sigma_{\theta y}(\Sigma_{\mathrm{hh}}^{-} + R)^{-1} \tag{10}$$

where $\Sigma_{\theta y}$ is the covariance matrix between Θ and y and Σ_{hh}^{-} is the prior covariance matrix of the model response for different quadrature realizations of Y. These expectations can be evaluated by the CUT approach. For example Σ_{hh}^{-} is approximately given by:

$$\Sigma_{\mathrm{hh}}^{-} \cong \sum_{q=1}^{N} w_q(h_q - \mu_{\mathrm{h}}^{-})(h_q - \mu_{\mathrm{h}}^{-})^T \tag{11}$$

where N is the number of quadrature points (425 in our case) and μ_{h}^{-} is the mean of the model response. We point out that $h_q$is the computed model response for the realization of Y corresponding to the quadrature point ξ_q.

4.2 *Posterior Moments*

Using the aforementioned framework, the posterior moments for the parameter vector is calculated. Due to the absence of true field measurements we use one of the realizations of Y as its true value and after polluting the corresponding acceleration time history with a Gaussian noise we get the measured response y in Equation (6). 50 randomly sampled time steps from the acceleration time history obtained from every sensor shown in Figure 1 is used, for each of the 425 runs, to compute the posterior moments according to Equations (8)-(11).

Table 2. Comparison between true value, prior and posterior means and standard deviations (SD).

RVs	True Value (MPa)	Prior Mean (MPa)	Post Mean (MPa)	Prior SD (MPa)	Post SD (MPa)
w_1	24.09	22.4	24.13	1.15	0.07
w_2	0.03	0.035	0.035	0.004	0.004
w_3	0.93	0.79	0.79	0.092	0.09
σ	4.32	3.70	3.65	0.43	0.32
σ_{xy}	4.32	3.70	3.70	0.43	0.42

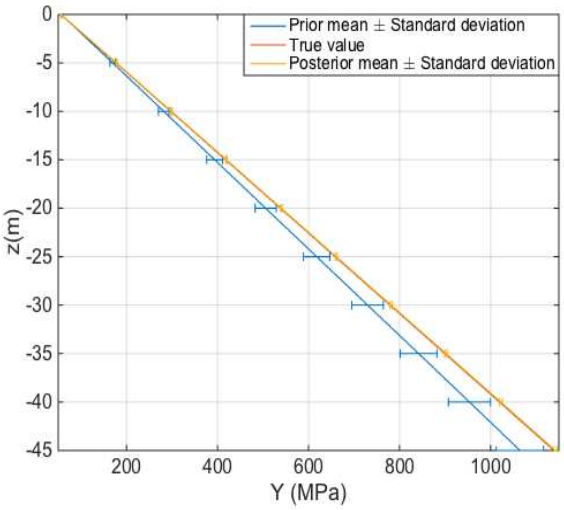

Figure 5. True value, prior mean and posterior mean and standard deviation of Young's modulus at (-5, -5, z).

5 RESULTS

The true values along with the prior and posterior moments of the random parameter vector, obtained after the inverse analysis, are listed in Table 2. We have also shown a comparison between the variation of prior mean, true value and posterior mean (with one standard deviation bound) of Y along depth at (x,y) = (-5,-5) in Figure 5. We can observe that the posterior mean of the Young's modulus is very close to the true value of Y with small error. In Figures 6 (a) and (b) we have shown the errors between the true value of Young's modulus distribution and the prior and posterior means respectively. In Figure 6 (c) the error between the posterior and the prior means of Young's modulus is plotted. Along with this an analysis to understand the information gain about the unknown parameters with respect to number of sensors and time steps was also conducted. In Figure 7 (a) the L_2-norm of error is plotted with respect to the number of time steps and sensors where error (e) is given by difference between the true value and posterior mean. For this we started by taking acceleration time history from sensors, along a line with offset 5 meter from source and depth 40m, in our analysis, and further added sensors while moving up the vertical direction. It was observed that the error decreases with increasing number of sensors and time-steps. An interesting thing to note is that the sensors bottom most layer did not contribute much to reducing error while the maximum error was reduced after inclusion of sensors from the surface. With this premise we went on to analyze the variation of $\Sigma_{\theta y}$across the soil domain, which represents the correlation of measurement data with random parameter vector $\boldsymbol{\theta}$. Since, from Equation (10), the Kalman gain matrix (K) is directly proportional to it, $\Sigma_{\theta y}$ gives us an idea about the amount of information gain at various locations in space. In Figure 7(b) we plot the trace of each column of $\Sigma_{\theta y}$ with respect to its spatial location for two different time instants. It can again be observed that amount of information gain decreases with increasing depth. An implication of this could be that only a few sensors located on and close to the surface give us almost all information about the domain. However further analysis on optimal location of sensor needs to be conducted to confirm this conjecture.

6 CONCLUSIONS

A methodology is developed to perform PDE-constrained stochastic waveform inversion using geophysical test measurements. It is illustrated by probabilistically characterizing a geotechnical site -- hypothesizing the Young's modulus of soil at the site to be a three-dimensional, heterogeneous, anisotropic random field and inversely estimating its parameters by using synthetic data from a fictitious geophysical experiment performed numerically at that site. Towards optimizing the number and locations of sensors in a geophysical experiment, a preliminary analysis is carried out using the developed methodology to. It is observed that the amount of information gain decreases with depth implying that the measurements at the bottom sensors do not contribute much to the inverse estimation process. The developed methodology is mathematically rigorous and computationally efficient. Moreover, it is general enough to be extended widely including inverse estimation of additional elastic as well as elastic-plastic soil parameters

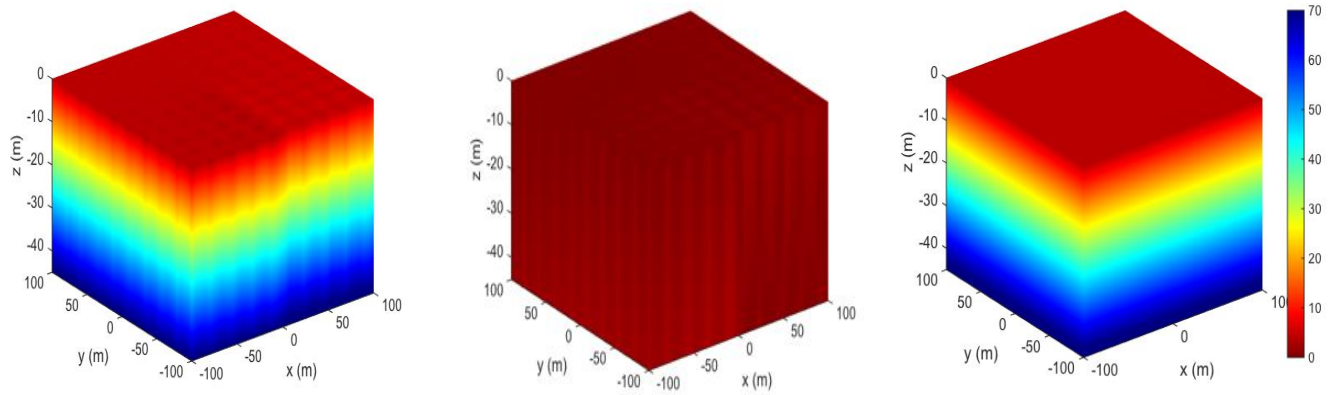

(a) (b) (c)

Figure 6. Spatial distribution of error between (a) prior mean of Young's modulus (MPa) and its true value, (b) posterior mean of Young's modulus (MPa) and its true value and (c) posterior and prior means of Young's modulus (MPa).

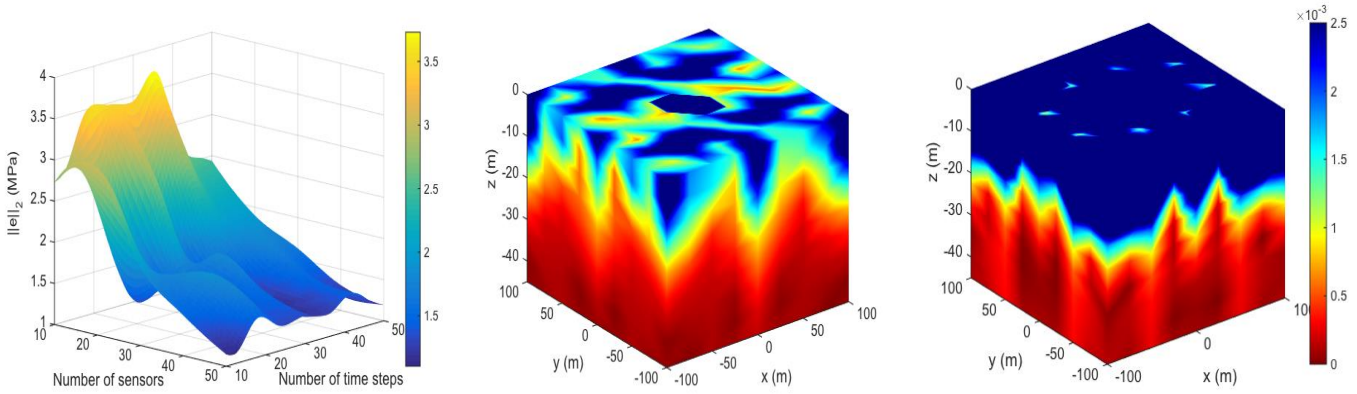

(a) (b) time = 4.5s. time = 5.5s.

Figure 7. (a) L_2-norm of error with respect to number of sensors and time steps, and (b) spatial distribution of $\Sigma_{\theta y}$ at 4.5s and 5.5s.

7 REFERENCES

Babuska, I.M., Nobile, F. & Tempone, R. 2007. A stochastic collocation method for elliptic partial differential equation with random input data. *SIAM Journal on Numerical Analysis* 43(3):1005-1134

Doucet, A., Freitas de, N. & Gordon, N. 2001. *Sequential Monte-Carlo Methods in Practice*. Springer-Verlag

Fathi,A. 2015. *Full-waveform inversion in three-dimensional PML-truncated elastic media: theory, computations and field experiments,* PhD Dissertation, The University of Texas at Austin

Ghanem,R.G. & Spanos,P.D.1991. *Stochastic finite elements:A spectral approach*, Springer

Kallivokas, L.F., Fathi, A., Kucukcoban, S., Stokoe K.H., Bielak, J. & Ghattas,O. 2013. Site Characterization using full waveform inversion. *Soil Dynamics and Earthquake Engineering* 47:62-82

Lacasse S. & Nadim F.1996. Uncertainties in characterizing soil properties. In Shackelford C.D.& Nelson,P.P.,(eds), *Uncertainty in Geologic Environment: From Theory to Practice, Proceedings of Uncertainty'96, July 31-August 3,1996,Madison, Wisconsin, Geotechnical Special Publication No. 58(1)*: 49–75 : ASCE, New York

Lysmer, J. & Kuhlemeyer, A.M. 1969. Finite dynamic model for infinite media, *Journal of the Engineering Mechanics Division*, ASCE 95: 859-877.

Iyengar,R.N. & Dash P.K. 1978. Study of the random vibration of nonlinear systems by the Gaussian closure technique. *Journal of Applied Mechanics* 45: 393–399

Madankan, R. 2014. *Model-data fusion and adaptive sensing for large scale systems:Application to atmospheric release*, PhD Dissertation, State University of New York at Buffalo.

Madankan, R., Pouget, S., Singla, P.,Bursik, M., Dehn, J., Jones, M., Patra, A.,Pavolonis, M., Pitman, E.B., Singh, T. & Webley, P. 2014. Computation of probabilistic hazard maps and source parameter estimation for volcanic ash transport and diffusion, *Journal of Computational Physics* 271:39-59

Nagavenkat, A.,2013. *The conjugate unscented transform - a method to evaluate multidimensional expectation integrals*, Master's thesis, State University of New York at Buffalo.

Nagavenkat, A., Singla P. & Singh T. 2012. The conjugate unscented transform-an approach to evaluate multi-dimensional expectation integrals, *Proceedings of the American Control Conference*

Nazarian,S. 1984. *In situ determination of elastic moduli of soil deposits and pavement system by Spectral-Analysis-of-Surface-Waves-method*, PhD Dissertation, The University of Texas at Austin